

# Mechanical and Electrical Properties of Multiwalled CNT-Alumina Nanocomposites Prepared by a Sequential Two-Step Processing of Ultrasonic Spray Pyrolysis and Spark Plasma Sintering

Kyubock Lee,<sup>‡</sup> Chan Bin Mo,<sup>§,\*</sup> Seung Bin Park,<sup>‡,†</sup> and Soon Hyung Hong<sup>§</sup>

<sup>‡</sup>Department of Chemical and Biomolecular Engineering, KAIST, 291 Daehak-ro, Yuseong-gu, Daejeon, 305-701, Korea

<sup>§</sup>Department of Materials Science and Engineering, KAIST, 291 Daehak-ro, Yuseong-gu, Daejeon, 305-701, Korea

The high tensile strength and electrical conductivity as well as high aspect ratio of carbon nanotube (CNT) are known to effectively improve the brittleness and electrical properties of ceramic materials; however, the agglomeration of CNTs during in the synthetic process and the poor interfacial bonding between CNTs and matrix materials still present challenges. Herein, multiwalled carbon nanotube (MWNT)-alumina composites were prepared, with homogeneously dispersed MWNTs in an alumina matrix, using a sequential two-step process via ultrasonic spray pyrolysis followed by a spark plasma sintering process. To mix these two materials at the molecular level, MWNT-alumina composites were prepared using a precursor solution containing Al ions instead of solid aluminum oxide particles as the starting material. The agglomeration of MWNTs at high concentration, which is a main obstacle to solution processing, was minimized using ultrasonic spray pyrolysis. The dc conductivity of pure  $\alpha$ -alumina, possessing substantial insulating properties, was increased to 12.2 S/m by incorporating 2.48 wt% of MWNTs with a low percolation threshold under 0.18 wt%. With the same amount of MWNT, the fracture toughness of the composite was increased 2.5 times. The improved electrical and mechanical properties of the composites are discussed based on the microstructural characteristics of the composites.

## I. Introduction

ALUMINA, due to its hardness as well as good chemical and thermal stabilities, is one of the most widely used ceramics. However, it has low fracture toughness, which is an intrinsic characteristic of ceramic materials, as well as low electrical conductivity. Therefore, if these properties of alumina can be improved, the ceramic would be expected to have a variety of possible applications.<sup>1–3</sup> The incorporation of a second phase, such as a metal, into the alumina matrix has been attempted to improve these drawbacks, although the improvements to the fracture toughness and electrical conductivity have not been sufficient.<sup>4</sup>

Carbon nanotubes (CNTs), due to their outstanding properties, have recently become fascinating materials as fillers for composite materials.<sup>1,5</sup> CNTs have a high Young's modulus, with good flexibility, high aspect ratio, high electrical conductivity, as well as good thermal and chemical stabilities.<sup>6</sup> However, there are still two main challenges in the

processing of CNTs as fillers; the homogeneous dispersion of CNTs in matrix materials and the interfacial bonding between the two different materials.<sup>3,7</sup>

CNTs tend to agglomerate easily due to their strong van der Waals interactions. The agglomerates of CNTs act as a critical defect in composites, which is undesirable for improving their mechanical and electrical properties.<sup>3,8</sup> In the fabrication of CNT-alumina composites, several approaches have been used to resolve this problem before the densification step via hot-pressing or spark plasma sintering (SPS). Physical mixing has been conducted under wet conditions to disperse CNTs into alumina powder, followed by ultrasonication and ball milling.<sup>9–14</sup> Chemical treatments have been performed on CNTs to obtain better uniformity of dispersion during colloidal processing.<sup>15,16</sup> The *in situ* growth of CNTs using chemical vapor decomposition onto alumina particles has been demonstrated to be more favorable process for obtaining composites with homogeneously distributed networks of CNTs.<sup>17,18</sup> All these processing methods are still associated with the problem of poor interfacial bonding between the CNTs and alumina matrix after densification, as solid alumina particles are used as the precursor for the alumina matrix. Therefore, intimate interfacial bonding between the surfaces of CNTs and oxide particles would not be expected. The sol-gel method has also been used to improve the poor interfacial bonding; however, the mechanical properties were not increased to the level expected.<sup>19</sup>

The synthesis of an alumina matrix from a precursor solution containing Al-ions was suggested by Cha *et al.* to allow intimate interfacial interactions between CNTs and the matrix, referred to as the molecular level mixing process.<sup>20</sup> Intimate interfacial bonding between two different materials has been successfully demonstrated to improved fracture toughness.<sup>20,21</sup> Moreover, Cha *et al.* showed that multiwalled CNTs (MWNTs) can improve the fracture toughness as much as single-walled CNTs (SWNTs). Most successful CNT-alumina composites had been obtained by combining SWNTs. However, MWNTs loadings of more than 1.8 vol% cause agglomeration of the MWNTs during the molecular level mixing process.<sup>20</sup>

Herein, an ultrasonic spray pyrolysis (USP) process has been proposed to prepare a MWNT-alumina composite from an aqueous precursor solution containing both MWNT and Al-ion as the precursor and to minimize the aggregation of the MWNTs. In the USP process, ultrasonic energy is applied to generate micron-sized droplets from precursor solution, which keeps good dispersion of MWNTs. In addition, it takes several seconds of short reaction time from precursor droplets to solid particles. These characteristics were helpful in preventing the MWNTs from agglomerating in the aqueous precursor solution. In this study, MWNT-alumina composites were densified into pellets using the SPS method. The hardness, fracture toughness, and

D. Marshall—contributing editor

Manuscript No. 28695. Received September 30, 2010; approved May 25, 2011.

\*Currently working at Samsung Electronics Co., Ltd.

<sup>†</sup>Author to whom correspondence should be addressed. e-mail: seungbinpark@kaist.ac.kr.

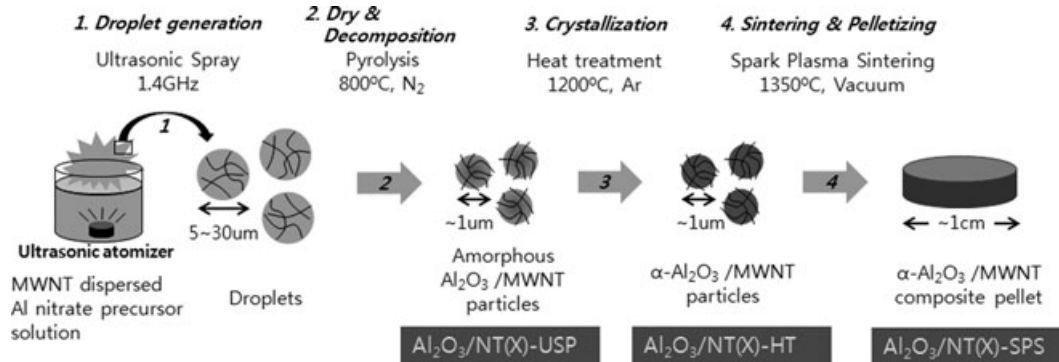


**Fig. 1.** Schematic illustration for the synthesis of MWNT-alumina composites. 1. Droplets containing MWNTs are generated from MWNTs-dispersed precursor solution by ultrasonic atomizer. 2. The precursor droplets are pyrolyzed in electric furnace at 800°C under N<sub>2</sub> atmosphere. Amorphous Al<sub>2</sub>O<sub>3</sub>/MWNT composite particles are synthesized in this step. 3. The particles were crystallized to be  $\alpha$ -Al<sub>2</sub>O<sub>3</sub>/MWNT composite particle by heat treatment at 1200°C under Ar atmosphere. Organic substances are decomposed in this step. 4. The particles are sintered and pelletized by spark plasma sintering at 1350°C under vacuum.

electrical conductivity of the MWNT-alumina composites were characterized.

## II. Materials and Methods

Multiwalled carbon nanotubes (CNT Co. Ltd., Incheon, Korea) were used as-received, without any further acid treatment or purification. Aluminum nitrate nonahydrate (Al(NO<sub>3</sub>)<sub>3</sub>·9H<sub>2</sub>O; Fluka, Buchs, Switzerland) and Pluronic P123 (HO(CH<sub>2</sub>CH<sub>2</sub>O)<sub>20</sub>(CH<sub>2</sub>CH(CH<sub>3</sub>)O)<sub>70</sub>(CH<sub>2</sub>CH<sub>2</sub>O)<sub>20</sub>H, BASF, Mount Olive, NJ) were used as a source of Al<sub>2</sub>O<sub>3</sub> and dispersing agent of the MWNTs, respectively. To prepare the precursor solution, 1 wt% of Pluronic P123 was dissolved in 80 mM of aluminum nitrate solution. Thereafter, a calculated amount of MWNTs, ranging from 0 to 2.5 wt% by theoretic yield, was dispersed in the precursor solution with the aid of a high energy tip sonicator (VCX 750; Sonics & Materials Inc., Newtown, CT). The MWNT-alumina composite particles were synthesized using an ultrasonic spray pyrolysis process. The MWNT-dispersed precursor solution was atomized into micron-sized droplets using an ultrasonic atomizer (frequency 1.7 GHz), and then passed to an 800°C electronic furnace with N<sub>2</sub> as a flow gas. The precursor droplets were dried and decomposed into submicrometer or micron-sized spherical particles along the quartz tube in the furnace. The prepared particles were crystallized into an  $\alpha$ -alumina phase, with the organic substance decomposed by heat treatment (HT) at 1200°C for 2 h under an argon atmosphere. After the HT, the MWNT-alumina composite particles were pelletized in a graphite mold to a diameter of 10 mm using the spark plasma sintering process (Dr. Sinter 1500 SPS; Sumitomo Coal Mining Co., Tokyo, Japan) at 1375°C under vacuum for 5 min.

In this study, the MWNT-alumina composites prepared from USP, HT or SPS are denoted as 'Al<sub>2</sub>O<sub>3</sub>/NT(X)-USP (or HT, SPS)'. 'X' denotes the amount of MWNTs in the alumina matrix by weight percentage (wt%) based on thermogravimetric analytical data. The electrical conductivity and mechanical properties of the composites were measured using the two-probe method and Vicker's indentation technique (five indentations on each material) under a load of 9.8 N, respectively. The fracture toughness was evaluated from the Antis equation, based on the crack lengths.<sup>22</sup>

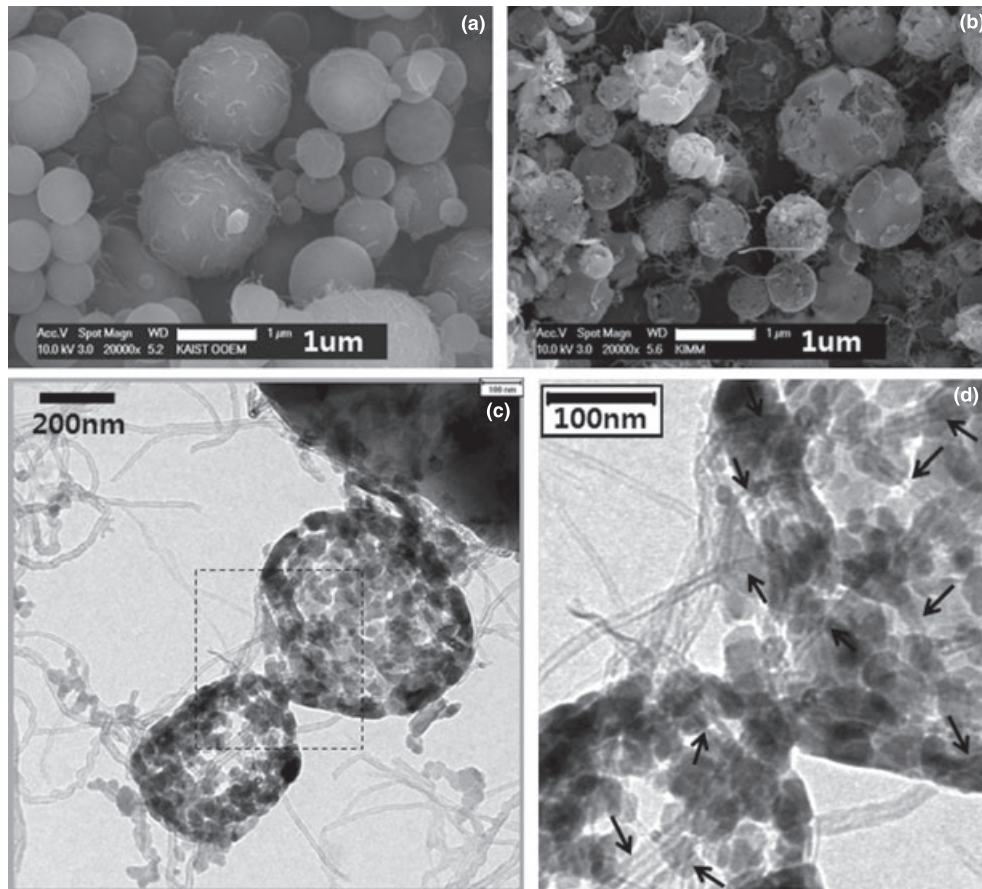
## III. Results and Discussion

Figure 1 shows the schematic illustration of the procedures for the synthesis of the MWNT-alumina composites. The generation of precursor droplets (step 1 in Fig. 1) and the dry/decomposition of the droplets (step 2) correspond to the USP process. The USP is advantageous for the preparation

of MWNT-ceramic composite particles from MWNT-dispersed aqueous precursor solution, without agglomeration of the MWNTs. In general, MWNTs are easily agglomerated in aqueous solution because of strong van der Waals interactions. For the successful dispersion of MWNTs in an aqueous solution, physical energy is needed in addition to the surface treatments, such as the incorporation of OH-functional groups or surfactants onto the MWNTs.<sup>8,23</sup> However, the dispersion of MWNTs is easily retarded by the addition of metal salts, such as aluminum nitrate, which makes the synthesis of MWNT-ceramic composites difficult when using the molecular level mixing process without agglomeration of the MWNTs. The dispersion of MWNTs into the precursor solution is maintained with the aid of ultrasonic energy, via an ultrasonic atomizer, for droplet generation. In addition, there was insufficient time for the MWNTs in the precursor droplets to agglomerate during the drying and pyrolysis processes as the reaction time of the droplet was <10 s.<sup>24</sup> In these experiments, the residence time of droplets in the reactor, obtained from the operating condition and dimensions of the setup (inner diameter of quartz tube, 50 mm; length of quartz tube, 1250 mm; flow rate of N<sub>2</sub>, 15 L/min), was calculated to be 9.8 s. This would be comparable to a reaction time of several hours using the other available solution processes, which leads to severe agglomeration of the MWNTs at certain concentrations.<sup>20</sup>

Figures 2(a) and (b) show SEM images of the composite particles after USP (step 2 in Fig. 1) and heat treatment (step 3), respectively. Submicrometer to micron-sized spherical MWNT-alumina composite particles, with an amorphous phase, were synthesized using USP [Fig. 2(a)]. The amorphous alumina was crystallized into  $\alpha$ -alumina via heat treatment [Fig. 3(a)]. The organic substances originated from the Pluronic P123 were simultaneously decomposed. As a result of the decomposition, pores were generated on the composite particles, as shown in Fig. 2(b). The final MWNT-alumina composite products, after carrying out SPS, contained little residual organic substances, as determined via thermogravimetry [TG; Fig. 3(b)] and differential scanning calorimetry (DSC; data not shown) analyses. The MWNTs were noted to be uniformly incorporated into the alumina matrix, as shown in Figs. 2(b-d). The arrows in the magnified TEM image shown in Fig. 2(d) indicate that the MWNTs were buried in the  $\alpha$ -alumina matrix.

Figure 4 shows the microstructures of the fractured surfaces of the MWNT-alumina composites after SPS (step 4 in Fig. 1). The grain sizes of the composites decreased with increasing amount of MWNTs, showing two important characteristics of the composites; the composites have good dispersion of MWNTs in the alumina matrix, with uniform grain sizes in each composite [Figs. 4(b-d)], and most of



**Fig. 2.** SEM image of (a)  $\text{Al}_2\text{O}_3/\text{NiO}(2.48)\text{-USP}$ , and (b) SEM and (c, d) TEM images of  $\text{Al}_2\text{O}_3/\text{NiO}(2.48)\text{-HT}$ . (d) is the magnified image of the part in (c) indicated by dashed line. MWNTs were well-dispersed in alumina matrix as indicated with arrows.

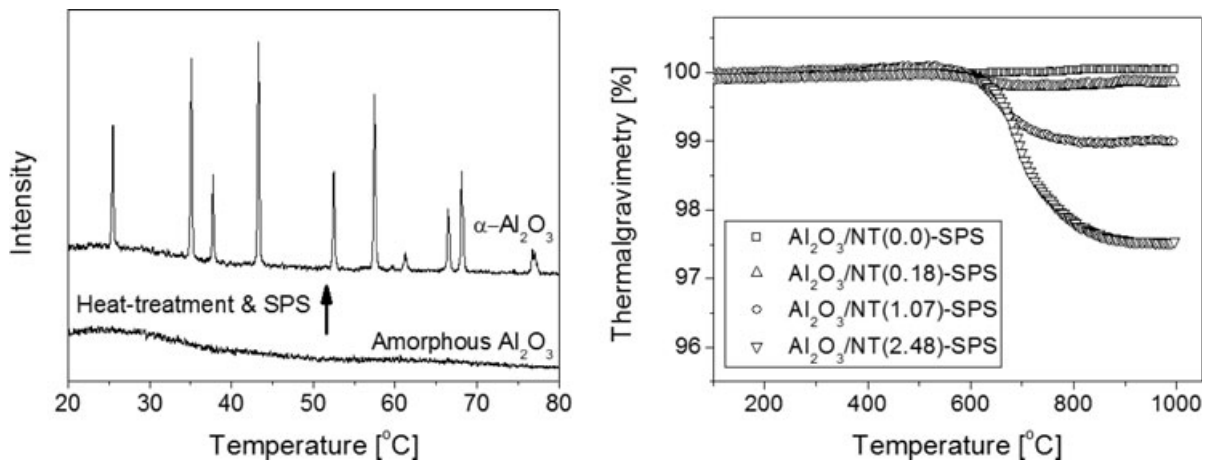


**Fig. 3.** (a) XRD analysis of  $\text{Al}_2\text{O}_3/\text{NiO}(2.48)\text{-USP}$  and  $\text{Al}_2\text{O}_3/\text{NiO}(2.48)\text{-SPS}$  and (b) TG analysis of  $\text{Al}_2\text{O}_3/\text{NiO}(X)\text{-SPS}$ . Amorphous phase of  $\text{Al}_2\text{O}_3/\text{NiO}(2.5)\text{-SP}$  was crystallized into  $\alpha\text{-Al}_2\text{O}_3$  phase [Figs. 2(b)–(d)] through heat treatment and SPS process.

the MWNTs were moved to the grain boundary of the alumina (Fig. 4), as shown in other previous studies.<sup>11,14</sup> This reveals that the interfacial energy between the MWNT and alumina was higher than that between the alumina grains. Even though some MWNTs were still observed to be incorporated inside the grains, as shown by the magnified images in Fig. 5, the composites cannot be considered to have the degree of expected chemically stable interfacial bonding between the MWNTs and alumina matrix.

The electrical and mechanical properties of the MWNT-alumina composites were closely related with the grain size and distribution of MWNTs. Figure 5(a) shows the dc conductivity of composites according to the amount of

MWNTs. The  $\alpha$ -alumina is known to be an electrical insulator. On the addition of <0.18 wt% MWNTs to the composite, an abrupt increase of the dc conductivity, by almost 12 orders of magnitude, the percolation threshold, which was comparable with the values reported in other studies (<0.7 vol%,<sup>15</sup>  $0.79 \pm 0.02$  vol%,<sup>9</sup> 0.18 wt% of MWNTs in  $\alpha$ -alumina matrix was calculated to be 0.55 vol%). The percolation threshold in composites with conductive spherical fillers is known to be around 16 vol%. This small percolation threshold value on the addition of MWNTs was attributed to high aspect ratio of the MWNTs.<sup>11,15</sup> In addition, most of the MWNTs in the alumina matrix were located at the grain boundary. This allowed even small amounts of MWNTs to

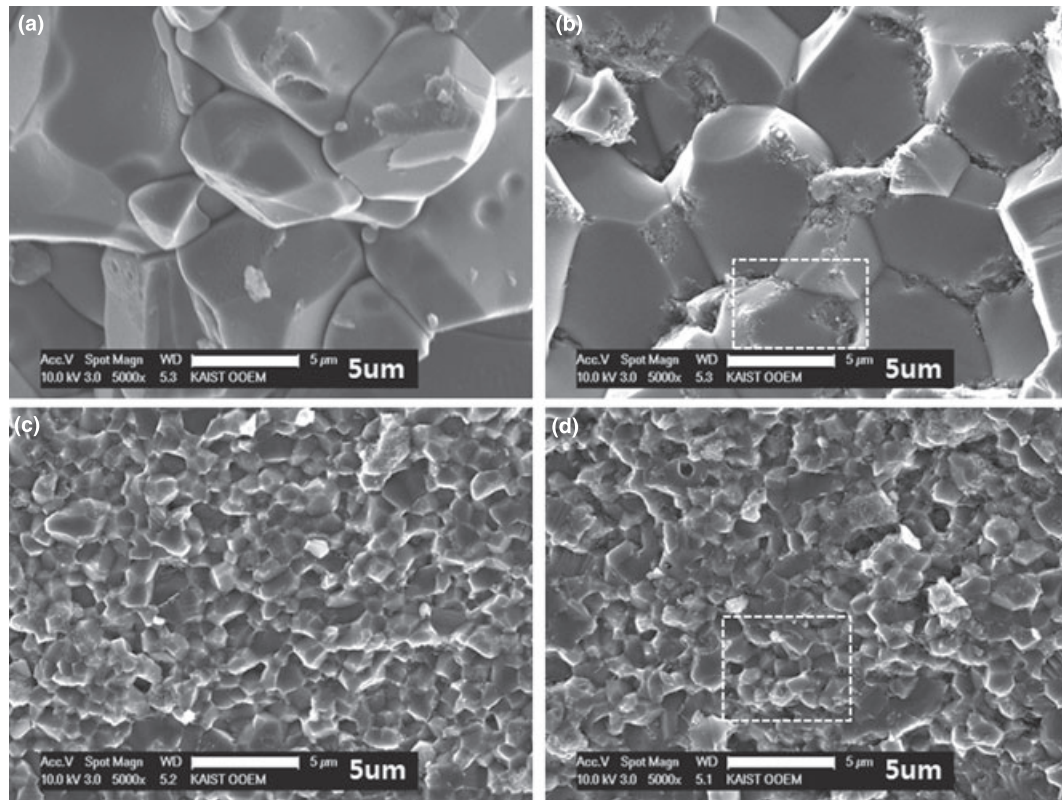


**Fig. 4.** SEM images of the fractured surfaces of (a)  $\text{Al}_2\text{O}_3/\text{NT}(0.0)\text{-SPS}$ , (b)  $\text{Al}_2\text{O}_3/\text{NT}(0.18)\text{-SPS}$ , (c)  $\text{Al}_2\text{O}_3/\text{NT}(1.07)\text{-SPS}$ , and (d)  $\text{Al}_2\text{O}_3/\text{NT}(2.48)\text{-SPS}$ . The grain sizes become smaller according to the amount of MWNTs in  $\text{Al}_2\text{O}_3$  matrix. MWNTs tend to be concentrated on the grain boundary.

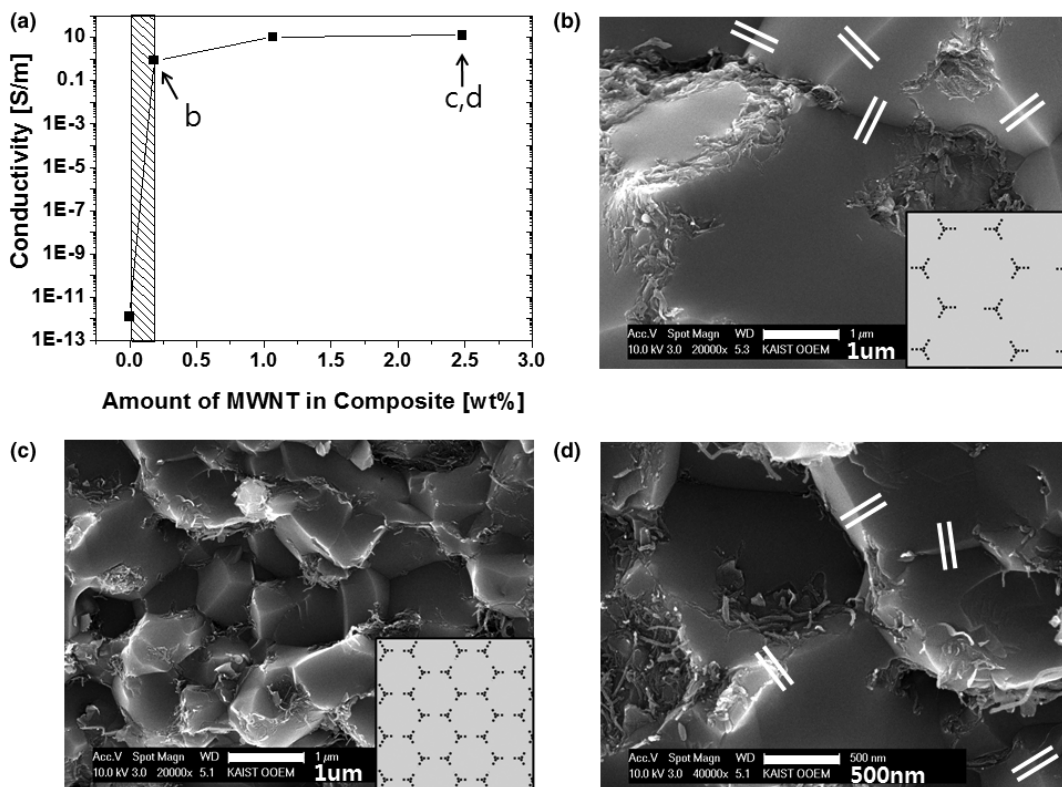


**Fig. 5.** (a) Electric conductivity of  $\text{Al}_2\text{O}_3/\text{NT}(x)\text{-SPS}$  plotted by the amount of MWNTs and the SEM images of fractured surfaces of (b)  $\text{Al}_2\text{O}_3/\text{NT}(0.18)\text{-SPS}$  and (c)  $\text{Al}_2\text{O}_3/\text{NT}(2.48)\text{-SPS}$ . Magnified SEM images of selected areas indicated by white dashed line in (b) Fig. 4(b) and (d) Fig. 4(d). (b, c) The most of MWNTs are distributed on the grain boundary. The distribution of MWNTs in (b) is sparse due to large grains of  $\text{Al}_2\text{O}_3$  crystals and small amount of MWNTs in comparison with (c). The increase of electric conductivity in accordance with the amount of MWNTs is explained by the illustration of inset image. MWNTs in (c) forms network in  $\text{Al}_2\text{O}_3$  matrix.

form a MWNT network for the path of an electron, as depicted in the inset to Fig. 5(b). The additional incorporation of 2.3 wt% MWNTs into the matrix above the percolation threshold did not increase the dc conductivity of the composite to the degree expected. This can be explained by the SEM images and schematically illustrated images of the fractured surfaces shown in Figs. 5(b–d). About 0.18 wt% of the MWNTs were not completely incorporated into the alumina matrix Au/Pt sputtering, as indicated by the double lines in Fig. 5(b). The further addition of MWNTs could not bridge the disconnection, but decreased the grain size; hence, the disconnection still remained as shown in Figs. 5(c) and (d). The mechanism of charge transport through the disconnected parts of the network has been explained using the concept of thermally induced hopping transport.<sup>9,25</sup> Even though hopping transport is thought to occur more effectively through the dense network of MWNTs in Al<sub>2</sub>O<sub>3</sub>/NT (2.48)-SPS than in Al<sub>2</sub>O<sub>3</sub>/NT(0.18)-SPS, the increased dc conductivity was <1 order of magnitude, as shown in Fig. 5(a). Inam *et al.*<sup>11</sup> reported that the electrical conductivity of a CNT-alumina composite was increased by increasing the grain size when the amount of CNT was fixed, as the density of CNT at the grain boundaries was increased. In addition, the electrical conductivity was increased by increasing the amount of CNT, but by maintaining a fixed grain size. These points clearly show that the electrical conductivity of a CNT-alumina composite is related to the CNT density at the grain boundary, which works as a conductive path.

Figures 6(a) and (b) show the hardness and fracture toughness of the MWNT-alumina composites according to the amount of MWNTs. On the addition of 2.48 wt% of MWNTs, the fracture toughness was increased by 152%; whereas, the hardness was decreased by 13%. Most previous studies on the mechanical properties of CNT-alumina composites have reported that increased fracture toughness is obtained by the addition of CNTs into the alumina matrix. However, no consensus on the hardness has been reached.<sup>3,13,14,18–20</sup> The SEM images shown in Figs. 6(b–d)

clearly demonstrate how the fracture toughness increases on the addition of MWNTs. The crack path of Al<sub>2</sub>O<sub>3</sub>/NT (2.5) exhibits a zigzag pattern [Fig. 6(d)]; whereas, that of Al<sub>2</sub>O<sub>3</sub>/NT(0) appears rather straight [Fig. 6(c)]. The pattern of the transgranular crack path in Al<sub>2</sub>O<sub>3</sub>/NT(0) shows a transition to an intergranular crack path on increasing the amount of MWNT. The grain size of the alumina decreased with increasing amount of MWNTs, and therefore more crack deflections would take place, which can retard the propagation of a crack [Fig. 4; Figs. 6(c) and (d)]. The frictional contact on the separating crack walls was also observed, as indicated by the white arrows in Fig. 6(d). The increased fracture toughness can also be explained by the energy-dissipating mechanisms. The black arrows in Figs. 6(d) and (e) indicate the MWNTs, which formed bridges across the crack and were pulled out on the fractured surface, respectively. When the composite cracked under an external load, a load transfer from the matrix to the MWNTs occurred. The energy absorbed by the fibers per unit area of composite was estimated using the following equation<sup>3</sup>:

$$G_{\text{pull-out}} = \frac{V_f L^2 \tau_i}{r},$$

where,  $V_f$  is the volume fraction of a fiber,  $r$  is the radius of a fiber,  $L$  is the length of a fiber, and  $\tau_i$  is the sliding shear stress. The thinner and longer CNTs are advantageous as toughening fillers, assuming that the volume fraction and sliding shear stress are fixed. A 200% increase in fracture toughness was reported when only SWNTs were used as fillers in the alumina matrix.<sup>13</sup> An increase in the fracture toughness of 152% shown in this study was remarkable considering that MWNTs were used. Even though the interfacial bonding between the MWNTs and alumina matrix would be sufficiently weak, with pulled out MWNTs easily found on

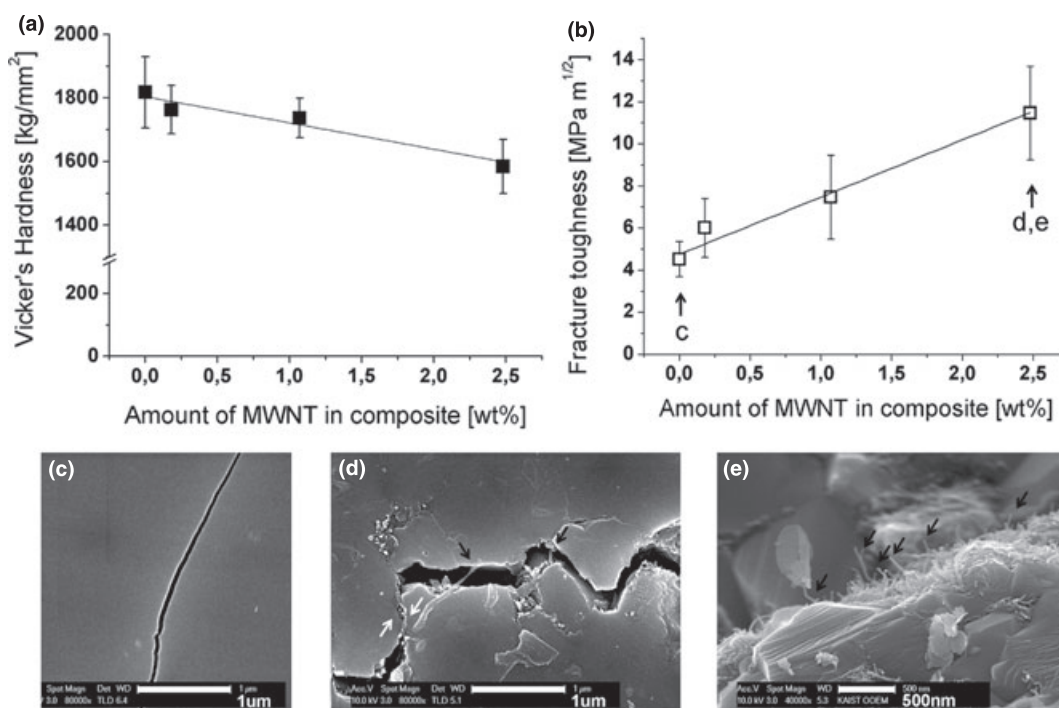


**Fig. 6.** (a) Hardness and (b) fracture toughness of MWNT-alumina composites plotted according to the amount of MWNTs in the composites. SEM images showing the crack propagation modes of (c) pure Al<sub>2</sub>O<sub>3</sub> (or Al<sub>2</sub>O<sub>3</sub>/NT(0.0)-SPS) and (d) Al<sub>2</sub>O<sub>3</sub>/NT(2.48)-SPS. The black and white arrows in (d) indicate MWNT bridges in the crack and the frictional contact on the separating crack walls, respectively. (e) Tilted SEM image of fractured surface showing pulled out MWNTs.

the fractured surface [Fig. 6(f)], MWNTs are considered to play a role of load transfer from the alumina matrix.

#### IV. Conclusions

A method for fabricating MWNT-alumina composites, using a sequential two-step process, via USP and SPS, has been proposed. Both the low percolation threshold value (<0.18 wt% or 0.55 vol%) in the dc conductivity and the increased fracture toughness of the composites by 2.5 times, were obtained from the homogeneous distribution of MWNT in the alumina matrix. The agglomeration of MWNTs at high concentrations was able to be minimized using the USP process, where ultrasonic energy was used for the generation of droplets from a precursor solution and only needs a short reaction time of a few seconds. The USP is a powerful process in the preparation of multicomponent or doped ceramic particles, with controllable chemical uniformity and stoichiometry, and therefore a number of applications would be expected for MWNT-ceramic composites designed using the USP process.

#### References

- <sup>1</sup>P. J. F. Harris, "Carbon Nanotube Composites," *Int. Mater. Rev.*, **49** [1] 31–43 (2004).
- <sup>2</sup>N. P. Padture, "Multifunctional Composites of Ceramics and Single-Walled Carbon Nanotubes," *Adv. Mater.*, **21** [17] 1767–70 (2009).
- <sup>3</sup>J. Cho, A. R. Boccacini, and M. S. P. Shaffer, "Ceramic Matrix Composites Containing Carbon Nanotubes," *J. Mater. Sci.*, **44** [8] 1934–51 (2009).
- <sup>4</sup>S. Hussain, I. Barbariol, S. Roitti, and O. Sbaizero, "Electrical Conductivity of an Insulator Matrix (Alumina) and Conductor Particle (Molybdenum) Composites," *J. Eur. Ceram. Soc.*, **23** [2] 315–21 (2003).
- <sup>5</sup>J. N. Coleman, U. Khan, and Y. K. Gun'ko, "Mechanical Reinforcement of Polymers Using Carbon Nanotubes," *Adv. Mater.*, **18** [6] 689–706 (2006).
- <sup>6</sup>V. N. Popov, "Carbon Nanotubes: Properties and Application," *Mater. Sci. Eng. R-Rep.*, **43** [3] 61–102 (2004).
- <sup>7</sup>A. V. Desai and M. A. Haque, "Mechanics of the Interface for Carbon Nanotube-Polymer Composites," *Thin-Walled Structures*, **43** [11] 1787–803 (2005).
- <sup>8</sup>L. Vaisman, G. Marom, and H. D. Wagner, "Dispersions of Surface-Modified Carbon Nanotubes in Water-Soluble and Water-Insoluble Polymers," *Adv. Funct. Mater.*, **16** [3] 357–63 (2006).
- <sup>9</sup>K. Ahmad, W. Pan, and S. L. Shi, "Electrical Conductivity and Dielectric Properties of Multiwalled Carbon Nanotube and Alumina Composites," *Appl. Phys. Lett.*, **89** [13] 133122 (2006).
- <sup>10</sup>J. P. Fan, D. Q. Zhao, M. S. Wu, Z. N. Xu, and J. Song, "Preparation and Microstructure of Multi-Wall Carbon Nanotubes-Toughened Al<sub>2</sub>O<sub>3</sub> Composite," *J. Am. Ceram. Soc.*, **89** [2] 750–3 (2006).
- <sup>11</sup>F. Inam, H. X. Yan, D. D. Jayaseelan, T. Peijs, and M. J. Reece, "Electrically Conductive Alumina-Carbon Nanocomposites Prepared by Spark Plasma Sintering," *J. Eur. Ceram. Soc.*, **30** [2] 153–7 (2010).
- <sup>12</sup>X. T. Wang, N. P. Padture, and H. Tanaka, "Contact-Damage-Resistant Ceramic/Single-Wall Carbon Nanotubes and Ceramic/Graphite Composites," *Nat. Mater.*, **3** [8] 539–44 (2004).
- <sup>13</sup>G. D. Zhan, J. D. Kuntz, J. L. Wan, and A. K. Mukherjee, "Single-Wall Carbon Nanotubes as Attractive Toughening Agents in Alumina-Based Nanocomposites," *Nat. Mater.*, **2** [1] 38–42 (2003).
- <sup>14</sup>S. C. Zhang, W. G. Fahrenholtz, G. E. Hilmas, and E. J. Yadlowsky, "Pressureless Sintering of Carbon Nanotube-Al<sub>2</sub>O<sub>3</sub> Composites," *J. Eur. Ceram. Soc.*, **30** [6] 1373–80 (2010).
- <sup>15</sup>M. Poorteman, M. Traianidis, G. Bister, and F. Cambier, "Colloidal Processing, hot Pressing and Characterisation of Electroconductive MWCNT-Alumina Composites With Compositions Near the Percolation Threshold," *J. Eur. Ceram. Soc.*, **29** [4] 669–75 (2009).
- <sup>16</sup>J. Sun, L. Gao, and X. H. Jin, "Reinforcement of Alumina Matrix With Multi-Walled Carbon Nanotubes," *Ceram. Int.*, **31** [6] 893–6 (2005).
- <sup>17</sup>J. W. An, D. H. You, and D. S. Lim, "Tribological Properties of hot-Pressed Alumina-CNT Composites," *Wear*, **255**, 677–81 (2003).
- <sup>18</sup>T. Zhang, L. Kumari, G. H. Du, W. Z. Li, Q. W. Wang, K. Balani, and A. Agarwal, "Mechanical Properties of Carbon Nanotube-Alumina Nanocomposites Synthesized by Chemical Vapor Deposition and Spark Plasma Sintering," *Compos. Part A-Appl. Sci. Manuf.*, **40** [1] 86–93 (2009).
- <sup>19</sup>C. B. Mo, S. I. Cha, K. T. Kim, K. H. Lee, and S. H. Hong, "Fabrication of Carbon Nanotube Reinforced Alumina Matrix Nanocomposite by Sol-Gel Process," *Mater. Sci. Eng. A-Struct.*, **395** [1–2] 124–8 (2005).
- <sup>20</sup>S. I. Cha, K. T. Kim, K. H. Lee, C. B. Mo, and S. H. Hong, "Strengthening and Toughening of Carbon Nanotube Reinforced Alumina Nanocomposite Fabricated by Molecular Level Mixing Process," *Scr. Mater.*, **53** [7] 793–7 (2005).
- <sup>21</sup>S. I. Cha, K. T. Kim, S. N. Arshad, C. B. Mo, and S. H. Hong, "Extraordinary Strengthening Effect of Carbon Nanotubes in Metal-Matrix Nanocomposites Processed by Molecular-Level Mixing," *Adv. Mater.*, **17** [11] 1377–81 (2005).
- <sup>22</sup>G. R. Anstis, P. Chantikul, B. R. Lawn, and D. B. Marshall, "Critical-Evaluation of Indentation Techniques for Measuring Fracture-Toughness. I. Direct Crack Measurements," *J. Am. Ceram. Soc.*, **64** [9] 533–8 (1981).
- <sup>23</sup>V. C. Moore, M. S. Strano, E. H. Haroz, R. H. Hauge, R. E. Smalley, J. Schmidt, and Y. Talmon, "Individually Suspended Single-Walled Carbon Nanotubes in Various Surfactants," *Nano Lett.*, **3** [10] 1379–82 (2003).
- <sup>24</sup>Y. C. Kang, S. B. Park, I. W. Lenggoro, and K. Okuyama, "Gd<sub>2</sub>O<sub>3</sub>: Eu Phosphor Particles With Sphericity, Submicron Size and Non-Aggregation Characteristics," *J. Phys. Chem. Solids*, **60** [3] 379–84 (1999).
- <sup>25</sup>B. E. Kilbride, J. N. Coleman, J. Frayssé, P. Fournet, M. Cadek, A. Drury, S. Hutzler, S. Roth, and W. J. Blau, "Experimental Observation of Scaling Laws for Alternating Current and Direct Current Conductivity in Polymer-Carbon Nanotube Composite Thin Films," *J. Appl. Phys.*, **92** [7] 4024–30 (2002). □